Theory of the Collapse of the Polyelectrolyte Brush

V. A. Pryamitsyn

Institute of Problems of Mechanical Engineering, Academy of Sciences of Russia, 61, Bolshoy pr., V. O., St-Petersburg, 199178, Russia

F. A. M. Leermakers* and G. J. Fleer

Department of Physical and Colloid Chemistry, Wageningen Agricultural University, Dreijenplein 6, 6703 HB, Wageningen, The Netherlands

E. B. Zhulina

Institute of Macromolecular Compounds, Academy of Sciences of Russia, 31, Bolshoy pr., V. O., St-Petersburg, 199004, Russia

Received May 30, 1996; Revised Manuscript Received August 19, 1996[⊗]

ABSTRACT: Both an asymptotic analytical analysis for chain length $N \rightarrow \infty$ and exact numerical calculations for finite chain lengths were applied to the structural properties of polyelectrolyte brushes under poor solvent conditions in a self-consistent field framework. We extend previous work on polyelectrolyte brushes and find evidence for a structural phase transition caused by internal phase separation in the polyelectrolyte brush upon a decrease of the solvent quality. In the limit of long chains, when a local electroneutrality approximation is exact, we find that the transition in the brush is continuous and tends to be second order. In the numerical calculations which employ the full Poisson−Boltzmann equation, a parameter window is found in which the structural phase transition is first-order. This is proven by the existence of a hysteresis loop in various properties of the brush, such as the degree of dissociation, the average height, the electrostatic potential profile, and the overall and end segment−density profiles. Apart from this difference as to the order of the transition, we find extremely good correspondence between the numerical calculations and the analytical asymptotic analysis for long polymer chains. The structure of the internally phase-separated layer is characterized by a condensed phase near the surface, a dilute swollen layer extending far into solution, and a thin interface between the two regions.

Introduction

Interfacial layers formed by end-grafted chains are recognized as fundamental features in many experimental systems. The layers are called brushes if the grafting density, i.e., the number of chains per unit area, exceeds the overlap threshold. In this limit, the excluded volume interactions cause the chains to stretch away from the interface. The effect is dramatic. For example, the height of the brush is known to scale linearly with the length of the chains.[1,2] Such thick layers are often necessary in issues related to colloidal stability. Polymer brushes in aqueous solutions are of special interest, for example, for environmental reasons. Many organic polymers are insoluble in water and cannot be used for these brushes. However, in this case one can use charged groups along the chain to improve the compatibility with water. Polyelectrolytes are therefore frequently used to influence the colloidal stability in aqueous systems.[3,4] Brushes composed of polyelectrolytes are now being studied systematically,[5−9] and several examples exist of naturally occurring polyelectrolyte brushes.[10,11] It is well-recognized that often polyelectrolytes are not water soluble if the charge is removed from the chain. In other words, the intrinsic polymer−solvent interactions are unfavorable for mixing; the uncharged polymer is under poor solvent conditions. For a special class of polyelectrolytes, polyacids, one can modify the charge of the chains by varying the pH of the solution. In such a system the solubility characteristics depend in a complex way on the conditions of the system.

Charged polymer brushes were studied recently by several groups of investigators.[6−9,12] Most work deals with brushes with a constant number of charges along the chain, sometimes called quenched polyelectrolytes. In that case the number of charges per chain can be varied by chemical means. We use a parameter, m, which is defined as the number of charges per chain divided by the chain length, N. For $m = 1$, one has a fully charged polymer. Indeed, there exists polymeric systems that have quenched characteristics, but more generally polyelectrolytes carry groups which can adjust the charge according to the local proton concentration. These are known as annealed polyelectrolytes, weak polyelectrolytes, or simply polyacids (polybases). We use the generic term polyacid for this type of system. In fact, it is more general to consider the polyacid system, as the quenched polyelectrolyte system is just a limiting case of the annealed one. For polyacids, there are two ways to control the charge density in the polyacid chain. The first one is to vary the number of (potentially) charged groups (i.e., the parameter m) in the same way as in the quenched polyelectrolyte case. The second way is to adjust the pH at a given m.

Recently, the structure of polyacid chains was analyzed theoretically by both analytical and numerical self-consistent field techniques.[6] For the polyacid brush in good solvents, nontrivial behavior of, for example, the rms (root mean square) brush height was found. It was shown that this height goes through a maximum as a function of the ionic strength. At very low ionic strength, the brush is only very weakly charged and the density profile of the inner part of the brush is parabola-like. At relatively high ionic strength, the brush is nearly neutral because the charges are screened by the salt,

[⊗] Abstract published in *Advance ACS Abstracts,* November 1, 1996.

S0024-9297(96)00783-8 CCC: $12.00

and the density profile of the brush is again parabolic. At an intermediate ionic strength a maximum is found in the (rms) average brush height.

As explained above, the good solvent case is not the most common condition. More frequently one will face the more complicated problem of a polyelectrolyte brush under poor solvency conditions. There is some history about the structure of the polyelectrolyte brush in poor solvents. Several years ago, it was claimed that the polyelectrolyte brush should show a first-order phase transition, which was unique because such a transition is not found in neutral brushes under variable solvent conditions.[8,13] These authors used a simple step-like model first suggested by Alexander.[1] However, this model is inadequate for the polyelectrolyte brush as has been shown by Misra *et al.*[7] They analyzed the quenched polyelectrolyte brush in the limit of infinitely long chains and found the transition to be second-order-like. We wish to examine this issue again, both with a detailed (semi)analytical approach and with full self-consistent field calculations with the model developed by Scheutjens and Fleer and extended to polyacid systems by Israëls *et al.* We will show that for finite chain lengths a first-order phase transition is possible.

The remainder of this paper is organized as follows. First we give some background information on the numerical theory. For details of this method we refer to the literature. Then full details of the analytical approach are given. In the results section we discuss predictions of both the analytical asymptotes and the numerical calculations for the polyacid brush in poor solvents. Conclusions will be formulated. In the Appendix some information is given about an extension of the brush theory for non-Gaussian chains.

Theory

Let us consider linear polyacid chains composed of N spherical symmetric units with a characteristic size, a. The chains are grafted with one end to an impenetrable, uncharged surface with a grafting density σ. The end-tethered chains form a brush in an aqueous 1−1 electrolyte (e.g., NaCl) solution, with a relative dielectric permittivity of 80. The ions and the water molecules are assumed to be of volume equal to that of the polymer units. Effectively we thus assume that the ions have a hydration shell and that the water is present as small clusters. The distance between acid groups of type HA along the chain is given by am^{-1}. We define an intrinsic pK value for the polyacid group and consider the equilibrium

$$\mathrm{HA} \overset{K}{\rightleftharpoons} \mathrm{H^+} + \mathrm{A^-} \qquad (1)$$

The local degree of dissociation $\alpha(x)$, where x is the distance away from the solid boundary, of the acid groups along the chain is controlled by the dissociation constant K and the local proton activity. $\ln K = -\Delta G/kT$, where ΔG is the Gibbs energy gain of the dissociation reaction and kT the thermal energy. Let us further consider the case that water is a poor solvent ($\chi > 0.5$) for the polyacid chains in its uncharged state (pH ≪ pK).

In the self-consistent field framework, the exact way to treat this system is by the Scheutjens Fleer (SF) formalism[14−16] as extended to weak polyelectrolytes by Israëls and co-authors.[12] In the formalism, a lattice is used which serves as a system of coordinates onto which the chain segments, the solvent molecules, and the ions are allowed to take positions. All possible and allowed chain conformations are taken into account by a Markov approximation (freely jointed chains). Short range (nearest neighbor) interactions are accounted for and parameterized by Flory−Huggins interaction parameters. Long range electrostatic interactions are included by the full Poisson−Boltzmann equation and implemented in a so-called multilayer Stern approach (ions can only take positions on lattice sites). The equations are then routinely solved numerically. Calculation times scale roughly linear with the chain length and are proportional to the size of the system. This allows calculations for (experimentally) rather realistic systems, but the limit of infinitely long chains can not be computed.

Lyatskaya *et al.* introduced an analytical theory for this problem.[6] Their work was based upon the framework of the parabolic potential profile and most likely trajectories for the chain conformations, as pioneered by Semenov.[17] They assumed that the brush is locally electroneutral, which is, strictly speaking, only correct in the limit of long chains. It was shown that this approximation is a good one even for rather short chains. The Gaussian model was used for the chain elasticity. This approach is not exact in the limit of strongly stretched chains (near the stretching limit) and thus the model of Lyatskaya *et al.* is formally not the exact asymptote of the SF formalism. Recently a scheme was developed which accounts for the finite extensibility of the chains[17−19] and which as we believe at present, is the exact limit of the SF formalism for very long chains. This modified analytical approach allows us to analyze the system characteristics for strongly stretched chains in the long chain limit. The main advantage of the (semi)analytical approach is that results can be generated at a fraction of the calculation time compared with the numerical theory. Thus, the analytical work can easily be used to sample the parameter space. This is an essential element in analyzing complicated systems such as the polyacid brush. In the following we will follow and generalize the analysis of Lyatskaya *et al.*

The starting point is the SCF formalism as introduced by Semenov[17] and the formulation of an expression for the free energy density of the brush. It is useful to specify first the distribution of the ions as a function of the distance x from the surface. It is assumed that all free ions differ from water only by the fact that they carry a charge. The short-range interactions are assumed to be the same as for water. Thus, there is only one Flory−Huggins interaction parameter, χ, which describes the interaction between the polymer units and all other entities in the system.

Volume fractions of the small entities in the brush at a distance x from the surface are denoted by the symbol $\rho_i(x)$, where i takes the values +1 (cations), 0 (water), or −1 (anions). Hence $\rho_0(x)$ is the distribution of the water molecules and, for example, $\rho_+(x) \equiv \rho_{+1}(x)$ is that of the cations (including the hydronium ions: H_3O^+, H^+). For the hydronium ions we need a special symbol because these affect the polymer charge; the density $\rho_{H_3O^+}(x)$ is abbreviated as $\rho_H(x)$. The concentrations of these components outside the brush are $\rho_i(\infty)$ and $\rho_H(\infty)$, respectively. Since the ionic strength in the bulk solution is often denoted as Φ, we define $\Phi_i = \rho_i(\infty)$, $\Phi_H = \rho_H(\infty)$, and $\Phi = \Phi_- + \Phi_+$, where again Φ_+ includes Φ_H.

In general, the ratio $\rho_i(x)/\Phi_i$ is determined by short range interactions, excluded volume effects, and elec-

trostatics. For water, the electrostatics play no role. We define a pseudopotential $\gamma(x)$ by

$$\rho_o(x) = \Phi_o \gamma(x) \quad (i = 0) \tag{2}$$

Obviously, $\gamma(x)$ depends on χ and on the local volume fraction $\rho_p(x)$ of polymer.[20]

For the ions an additional electrostatic factor, $y(x) \equiv \exp(-e\psi(x)/kT)$, enters; here $\psi(x)$ is the electrostatic potential, e the elementary charge, and kT the thermal energy. Hence we can write

$$\rho_i(x) = \Phi_i \gamma(x)(y(x))^i \quad (i = -1, i = +1) \tag{3}$$

In order to find the electrostatic potential $\psi(x)$ and the corresponding distributions of ions, we should in principle solve the Poisson−Boltzmann equation, as is done in the SF approach. The disadvantage is that then no analytical progress can be made. Here we adopt a simplified approach known as the local electroneutrality approximation (LEA). This approach has been validated for the case where the height of the brush considerably exceeds the Debye screening length for electrostatic interactions. The LEA concept assumes a complete compensation of the charge due to the dissociated segments of the polyacid by the charges of the mobile ions at each point in the brush, such that the total charge density is zero everywhere. If $\alpha(x)$ is the local degree of dissociation of the brush segments, the polymer charge density is $-m\alpha(x)\rho_p(x)$. Hence, in the LEA we have

$$m\alpha(x)\rho_p(x) + \rho_-(x) = \rho_+(x) \tag{4}$$

In the bulk, the volume fraction of water will be $1 - \Phi$. Equation 4 can be rewritten with the help of eq 3 in the form

$$m\alpha(x)\rho_p(x) + \frac{\Phi}{2}\frac{\gamma(x)}{y(x)} = \frac{\Phi}{2}\gamma(x)\, y(x) \tag{5}$$

where we used the electroneutrality condition $\Phi_- = \Phi_+ = \Phi/2$ for the bulk.

The approximation imposed on the distribution of charges as expressed in eqs 4 and 5 implies that the electrostatic interactions are strong. The ions are forced to enter the brush and compensate the brush charge. Another way to look at it is that when the local charge created by the dissociation of the polymer segments is high, the electrostatic potential is locally adjusted such that the counterions are imported and the co-ions expelled such that the brush charge is exactly compensated. Thus the local electrostatic potential is coupled to the charge density of the polymer units. There is a slight inconsistency in the model because Poisson law states that $\partial^2\psi/\partial z^2$ is related to the local excess charge δq. From the general theory for the polymer brush, we know that, in the limit of large chains, all structural functions of the brush become universal functions of the normalized dimensionless distance $z = x/(aN)$. This means that the local charge density $\delta q \sim N^{-2}\, \partial^2\psi/\partial z^2$ tends to go to zero as N^{-2}. We also know that the brush height, H, scales as N, and as the electrostatic potential in the brush is finite, we find that the electrostatic contribution to the free energy is proportional to $H\delta q\langle\psi\rangle$, and therefore the electrostatic part of the free energy scales as N^{-1}. Thus, with diverging N the local electroneutrality approximation becomes exact. In effect, we abandon the Poisson−Boltzmann equation in the analytical approach and replace it by the electroneutrality constraint and realize that the result is applicable in the long chain length limit. The local electroneutrality ansatz is completely analogous to calculating the equilibrium distribution of ions and the electrostatic potential in a classical Donnan equilibrium.

The free energy for the SCF approach should be written as the sum of an elastic term and a mixing term.

$$\frac{F}{kT} = -\frac{S_{el}[\rho_p]}{k} + \int_0^\infty f(\rho_p)\, dx \tag{6}$$

where S_{el} is the conformational entropy of the polymer chains which is only a functional of the polymer density profile. The second contribution in eq 6 is the local (normalized) free energy density which is a function of the distribution of the polymer units, the degree of dissociation and the ion distributions including that of the protons; it includes short and long range (electrostatic) interactions, but no chain elasticity. Both contributions collected in eq 6 are already discussed by Lyatskaya *et al.*[6] With respect to this work, in our system we only have to add the term due to short range interactions which expresses the solvent quality for the polymer units. The local free energy density, expressed in units of kT per unit volume (i.e., the volume of a polymer segment), is given by

$$\begin{aligned} f(\rho_p(x),\alpha(x),\rho_+(x),\rho_-(x),\rho_0(x)) = \\ m\rho_p(x)\Big[\alpha(x)\ln\alpha(x) + (1-\alpha(x))\ln(1-\alpha(x)) - \\ \alpha(x)\ln\frac{K}{\Phi_H}\Big] + \rho_+(x)\ln\rho_+(x) - \rho_+(x)\mu_+ + \\ \rho_-(x)\ln\rho_-(x) - \rho_-(x)\mu_- + \rho_0(x)\ln\rho_0(x) - \\ \rho_0(x)\mu_0 + \rho_p(x)\chi(1-\rho_p(x)) \end{aligned} \tag{7}$$

In this equation μ_+, μ_-, and μ_0 are Lagrange multipliers coupled to the condition that outside the brush, where $\rho_p = 0$, the density of the co-ions and counterions equal $\Phi/2$ and that the density of water equals $1 - \Phi$. These Lagrange multipliers are a function of the chemical potentials of the ions and of the density of water in the bulk, respectively. If the density of the ions in the bulk is known, the amount of water will automatically be known if we impose the condition that the sum of the densities equals unity, which corresponds to the incompressibility constraint:

$$\rho_0(x) = 1 - \rho_p(x) - \rho_+(x) - \rho_-(x) \tag{8}$$

The terms $\alpha \ln \alpha$ and $(1 - \alpha)\ln(1 - \alpha)$ describe the mixing entropy of charged and uncharged groups. The K/Φ_H term is the reference free energy for the dissociation of the acid groups.[21] The term $\rho \ln \rho$ is associated with the translational entropy of the mobile ions and the water molecules. Finally, the last term of eq 7 expresses the polymer−solvent interactions. As noted above, we assume that the polymer units interact identically with all other components in the system. Thus, only one Flory−Huggins interaction parameter is needed. Due to the electroneutrality approximation, f does not contain any explicit electrostatic terms, which is allowed as discussed above for systems with long grafted chains. The electrostatic interactions are still accounted for because $\alpha(x)$ is coupled to $y(x)$ through eq 5. Also, the degree of dissociation is coupled to K and to the pH. When a polymer unit is under zero electro-

static potential, for example, in the bulk, we have where

$$\frac{K}{\Phi_H} = \frac{\alpha_b}{1-\alpha_b} \tag{9}$$

$\Phi_H = 10^{-pH}$ and α_b is the degree of dissociation of an acid unit in the bulk.

It is possible to reduce the number of parameters in eq 7. The density of the water molecules can be eliminated by eq 8, and the density of for example the cations can be eliminated with the help of eq 4:

$$f(\rho_p,\alpha,\rho_-) = m\rho_p\left[\alpha \ln \alpha + (1-\alpha)\ln(1-\alpha) - \alpha(x)\ln\frac{K}{\Phi_H}\right] + (m\alpha\rho_p + \rho_-)\ln(m\alpha\rho_p + \rho_-) - (m\alpha\rho_p + \rho_-)\ln\frac{\Phi}{2} + \rho_-\ln\rho_- - \rho_-\ln\frac{\Phi}{2} + (1 - (1+m\alpha)\rho_p - 2\rho_-)\ln(1-(1+m\alpha)\rho_p - 2\rho_-) - (1-(1+m\alpha)\rho_p - 2\rho_-)\ln(1-\Phi) + \rho_p\chi(1-\rho_p) \tag{10}$$

where $\rho_p = \rho_p(x)$, $\alpha = \alpha(x)$, and $\rho_- = \rho_-(x)$.

In order to differentiate the free energy density with respect to the polymer volume fraction, we first need to minimize eq 10 with respect to α and ρ_-. The minimization with respect to α leads to

$$\frac{\alpha}{1-\alpha} = \frac{\alpha_b}{1-\alpha_b}\frac{\Phi}{2(1-\Phi)}\frac{(1-(1+m\alpha)\rho_p - 2\rho_-)}{m\alpha\rho_p + \rho_-} \tag{11}$$

The minimization with respect to the anion density gives

$$\rho_- = \left(\frac{\Phi}{2(1-\Phi)}\right)^2 \frac{(1-(1+m\alpha)\rho_p - 2\rho_-)^2}{m\alpha\rho_p + \rho_-} \tag{12}$$

Equations 11 and 12 constitute two equations in three unknowns, $\alpha(x)$, $\rho_p(x)$, and $\rho_-(x)$. Two of them can be eliminated, and f can then be written as a function of the third. It turns out that it is most convenient to retain $\alpha(x)$ as the variable to parameterize, $f(\rho_p(\alpha))$. The result is

$$\rho_p = [\Phi(\alpha_b - \alpha)(\alpha_b + \alpha(1-2\alpha_b))]/[\alpha_b{}^2\Phi + \alpha\alpha_b{}^2\Phi(m-2) + \alpha^2[mA_b + \Phi(A_b - 1)] + \alpha^3 m[A_b + \Phi]] \tag{13}$$

$$\rho_- = [m\Phi\alpha^3(\alpha_b - 1)^2]/[\alpha_b{}^2\Phi + \alpha\alpha_b{}^2\Phi(m-2) + \alpha^2[mA_b + \Phi(A_b - 1)] + \alpha^3 m[A_b + \Phi]] \tag{14}$$

where again $\alpha = \alpha(x)$ and where we have introduced $A_b \equiv 2\alpha_b(1-\alpha_b)$.

As shown before (see, for example, refs 21−26 and the Appendix), the minimum of the total free energy of the brush with respect to ρ_p is defined by

$$u[\rho_p(x)] = \Lambda - V\left(\frac{x}{aN}\right) \tag{15}$$

where $V(z)$ is a function of a dimensionless distance $z = x/(aN)$ and u is the exchange chemical potential which will be addressed below. The function $V(z)$ depends only on the mechanism of the extensibility of the polymer chains. In the literature, usually the Gaussian model is applied, according to which

$$V_{Gaussian}(z) = \frac{3\pi^2 z^2}{8} \tag{16}$$

We will use a more exact model for the mechanism of the chain extensibility.[18] In the Gaussian model, it is possible that chains extend further than their physical length, which is not realistic. We use the model of freely jointed chains on a body centered cubic lattice (BCC). For this model we find (see the Appendix):

$$V_{BCC}(z) = -3\ln\left(\cos\frac{\pi z}{2}\right) = \frac{3\pi^2}{8}z^2 + \frac{\pi^2}{64}z^4 + \ldots \tag{17}$$

From the Taylor expansion of $V_{BCC}(z)$ as given in eq 17 it is clear that the Gaussian result is recovered as the first term. Also, for $z = 1$, $\cos(\pi z/2) = 0$, which causes V_{BCC} to diverge, which is realistic for "real" chains. It was found that the Gaussian model is good when $z < 0.5$ and that corrections as given in the BCC approach become more important for $z > 0.5$. In general, the Gaussian model includes an artificial tail to the density distribution (even for long chains).

In eq 15, Λ is a normalization constant defined by the condition that

$$\int_0^H \rho_p(x)\,dx = \sigma N \tag{18}$$

where H is the height of the brush and σ the grafting density. When

$$\partial f(\rho_p,\rho_-,\alpha)/\partial\alpha = \partial f(\rho_p,\rho_-,\alpha)/\partial\rho_- = 0$$

$$\frac{\partial f(\rho_p,\rho_-,\alpha)}{\partial\rho_p} \equiv \frac{\partial f(\rho_p)}{\partial\rho_p} = u(\rho_p) \tag{19}$$

Hence, $u(\rho_p)$ can be obtained from

$$\partial_f/\partial\rho_p = (\partial f/\partial\alpha)(\partial\alpha/\partial\rho_p)$$

where the first factor is found from substituting eqs 13 and 14 into eq 10 and differentiation with respect to α, and the second from differentiating eq 13. The result is

$$u(\rho_p,\rho_-,\alpha) = m\alpha\ln\left[\frac{2\alpha(1-\alpha_b)(1-\Phi)(m\alpha\rho_p + \rho_-)}{\alpha_b(1-\alpha)\Phi}\right] + m\ln[1-\alpha] - (1+m\alpha)\ln[1-(1+m\alpha)\rho_p - 2\rho_-] - 2\chi\rho_p \tag{20}$$

Equations 13−20 allow us to calculate the density profiles of the polyacid brush. In the BCC approach, the polymer density profile should follow from

$$u[\rho_p(x)] = \Lambda + 3\ln\cos\left(\frac{\pi z}{2}\right) \tag{21}$$

Thus the density profile $\rho_p[u]$ can be obtained from the inversion of eq 21. This inversion is possible when the function $u[\rho]$ is a monotonous function. In poor solvents this is not guaranteed and the system will need a special treatment.

Conditions for Phase Equilibrium within the Brush

In Figure 1 we show the segment potential as a function of the polymer density for two values of the Flory−Huggins interaction parameter χ. From this

figure it is clear that for low values of χ the function is monotonous, which means that there is only one potential corresponding to one density. However, for a larger value of χ, this is no longer the case. There can be more values for the polymer density that correspond to a given segment potential. We find a loop in $u[\rho_p]$, for example, for $\chi = 1$, which is characteristic for phase coexistence. In such a case we need to specify the correct criteria to cut this loop into sections. Within such a section the polymer density, ρ_p, is a unique function of segment potential, u. When the boundaries of these regions are determined, we can solve analytically the above set of equations for each region.

We should realize that locally in the polymer brush, where the polymer density is ρ_p, the polymer should behave similarly to a homogeneous polymer solution of infinitely long chains at that polymer density ρ_p. The limit of infinitely long chains is used because u contains the local properties of the brush. A solution of infinitely long chains does not contain contributions due to translational entropy and is only a function of local terms. For such a homogeneous polymer solution it is possible to define a partial pressure:

$$\pi[\rho_p] = -\left(\frac{\partial F}{\partial V}\right)_n = -\left(\frac{\partial F/n}{\partial V/n}\right)_n = -\left(\frac{\partial \frac{f}{\rho_p}}{\partial \frac{1}{\rho_p}}\right)_n = -f[\rho_p] + \rho_p u[\rho_p] \quad (22)$$

where F is the free energy of the homogeneous polymer solution, f the free energy density, n the number of monomers, and $u = \partial f/\partial\rho$ a segment chemical potential. The expression for f is given in eq 10 when the dependence of x is dropped. To return to the brush system, we obtain the local lateral pressure in the brush corresponding to the partial pressure of the homogeneous polymer system of infinitely long chains of concentration $\rho_p(x)$:

$$\pi[\rho_p(x)] = f[\rho_p(x)] + \rho_p(x)u[\rho_p(x)]$$

The segment chemical potential and the lateral pressure should be continuous functions of the x coordinate. Thus, we produce the binodal conditions

$$\pi[\rho_p^{(1)}] = \pi[\rho_p^{(2)}]$$
$$u[\rho_p^{(1)}] = u[\rho_p^{(2)}] \quad (23)$$

where 1 and 2 are labels referring to the two coexisting phases. Thus when a loop is present for $u(\rho_p)$ the brush jumps in density from $\rho^{(1)}{}_p$ to $\rho^{(2)}{}_p$ at the point where $u[\rho^{(1)}{}_p] = u[\rho^{(2)}{}_p] = u_b$. In Figure 1 an example is given. Note that the conditions as specified by eq 23 correspond to an equal area argument: the area above u_b and below u_b in the loop should be equal. In the present system it is possible to find the transition point numerically.

Results

Above we have given an outline of the numerical model and given all the details needed to understand the analytical asymptotics. In this section we will discuss the two SCF approaches simultaneously. The analytical model (implying the $N \to \infty$ limit) is used (i) to examine the conditions for an internally phase-separated brush and (ii) to obtain the phase diagram for the annealed polyelectrolyte brush in poor solvent.

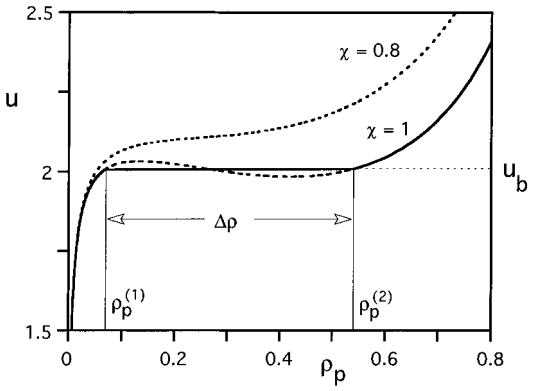

Figure 1. The segment chemical potential as a function of the polymer density of a homogeneous polyacid solution with infinite chain length. Parameters: $\Phi = 0.001$, $\alpha_b = 0.9$, $m = 1$.

Before we analyze the phase transition itself, we compare numerical and analytical predictions for the density profiles of an internally phase separated brush.

Phase Diagram. In Figure 1 an example was given on how to find the binodal points of the internally phase-separated brush: (i) calculate the potentials as a function of the density and (ii) use the Maxwell rule to find the transition densities. This method is used to obtain the binodal densities as a function of the χ parameter (inverse temperature) for various values of the ionic strength and the pH. Instead of specifying the pH, it is convenient to use the degree of dissociation α_b of the polymer units in the absence of an electrostatic potential. When $pK \ll$ pH, $\alpha_b = 1$; when $pK =$ pH, $\alpha_b = 0.5$; and when $pK \gg$ pH, the polymer is uncharged ($\alpha_b = 0$).

A collection of binodals is presented in Figure 2. The usual shape of phase coexistence curves is found. The stable one-phase systems are situated on the outside, for compositions that correspond to the inside of the U-shaped region, the system is unstable. An unstable composition phase separates into a dilute polymer phase in equilibrium with a phase with high polymer density. The lowest point on the coexistence curve corresponds to the critical point specified by (ρ_p^{cr},χ^{cr}). In the examples given in Figure 2, the binodal curves are asymmetric, with the critical point shifted to the low side of the polymer density. It is possible to create a symmetric binodal in the limiting case of high charge ($\alpha_b = 1$) and low ionic strength in very bad solvents (not shown). Moreover, it would then be needed to neglect the volume of the ions in order not to dilute the collapsed polymer phase.

The position of the critical point is defined by

$$\frac{\partial u}{\partial \rho_p} = \frac{\partial^2 u}{\partial \rho_p^2} = 0 \quad (24)$$

For general conditions of Φ, α_b, and m, there is no easy solution of eq 24. However, in the limit of zero ionic strength $\Phi \to 0$ (in a model with finite volume of the ions) and for the strong polyelectrolytes ($\alpha_b \to 1$) the following simple result is obtained:

$$\rho_p^{cr} = \sqrt{\frac{m}{1+m}}\left(1 - \sqrt{\frac{m}{1+m}}\right) \quad (25)$$

$$\chi^{cr} = \frac{1}{2} + \frac{3}{2}m + m^2 + \sqrt{m(1+m)^3}$$

When $m = 0$ we have $(\rho^{cr}{}_p,\chi^{cr}) = (0, {}^1/_2)$ which is the

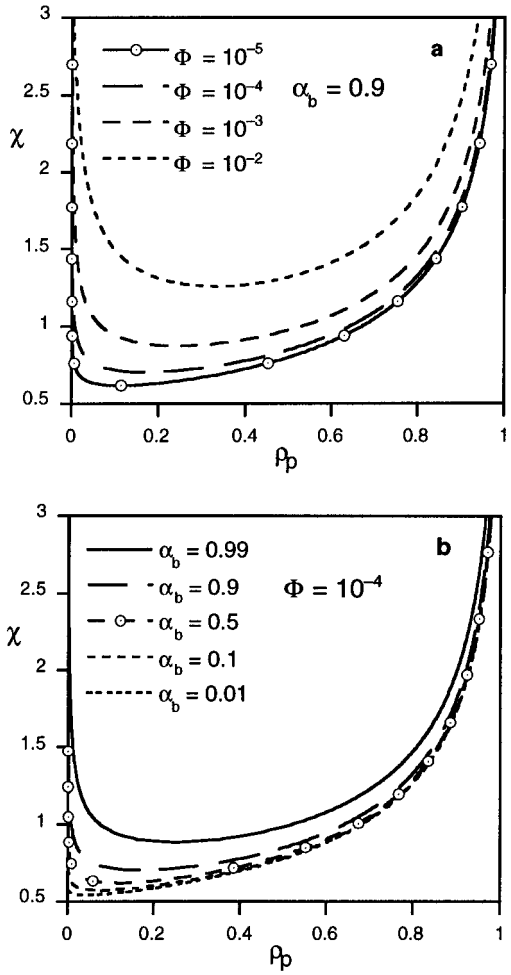

Figure 2. Binodals (phase coexistence curves) of polyacid solution of infinitely long chains for (a) various ionic strengths and fixed degree of dissociation α_b and (b) various degrees of dissociation and constant ionic strength as indicated. The binodals are calculated in a homogeneous polyelectrolyte system, $m = 1$, where no gradients in electrostatic potential are present.

limit for long neutral polymers, as known from the Flory−Huggins theory. Inspection of eq 25 shows that ρ^{cr}_p will always be relatively low. In the limit of $m \to 0$, $\rho^{cr}_p = 0$ and when $m \to 1$, we find that $\rho^{cr}_p = {}^1/_2(\sqrt{2} - 1)$. We find that ρ^{cr}_p goes through a maximum as a function of the fraction of charges, m, in the chain. This maximum is situated at $m = {}^1/_3$ (every third segment along the chain is charged), for which $(\rho^{cr}_p, \chi^{cr}) = ({}^1/_4, 2)$. This point serves as an upper limit for ρ^{cr}_p in the zero ionic strength limit.

Realistic values of the parameters thus lead to asymmetric binodals. Inspection of Figure 2 reveals that the interaction parameters for which we obtain an internally phase-separated brush layer are not extremely high and they are well within the experimental range. The behavior of the critical point as a function of the ionic strength and α_b is rather complicated. It is possible to find almost the same curve for rather different values of the ionic strength and α_b (see the two marked lines in Figures 2a,b which coincide except for very low density); a low ionic strength can be compensated by a high degree of dissociation. Obviously, when $\alpha_b \to 0$, the binodal becomes independent of ionic strength. For relatively high ionic strength and high degree of dissociation the critical point is found at relatively high interaction parameters. In this case it is possible to have a measurable finite concentration in the dilute branch of the phase coexistence. Below we will show examples of systems with these characteristics.

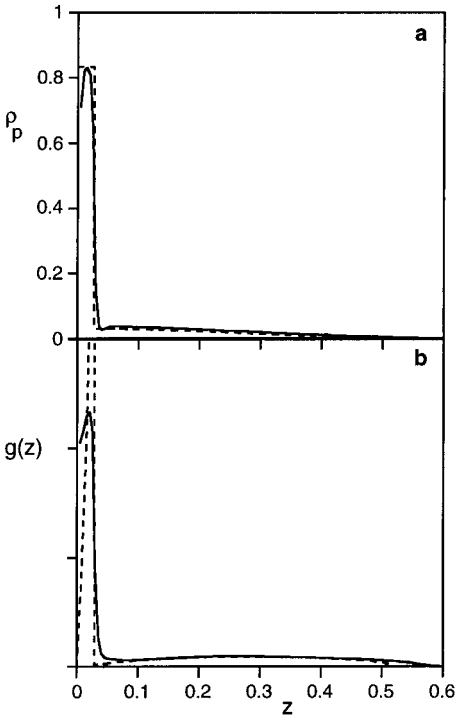

Figure 3. (a) Overall density profile as a function of the normalized dimensionless distance $z = x/(aN)$ with $N = 200$. (b) End-point density as a function of z. The results for the numerical model are given by the solid curves and the results for the asymptotic analytical model are given by the dashed curves. Parameters: $\Phi = 0.01$, $\alpha_b = 0.9$, $\sigma = 0.03$, $\chi = 2$, $m = 1$.

For a finite ionic strength the binodals have an endpoint at $\rho_p = 0$ for finite values of χ. The intersection with the χ-axis is found by the condition that the partial pressure equals zero. After this, the right branch of the binodal is found by the condition of zero partial pressure. The difference of the two marked lines in Figure 2 with respect to the intersection of the χ-axis is rather large, which is seen by the marks on the *y*-axis continuing further for the system with lowest ionic strength. Thus the maximum χ value for which there is a swollen tail in equilibrium with a condensed phase is a decreasing function of the ionic strength.

Density Profile for an Internally Phase-Separated Polyelectrolyte Brush. Once the binodal values are located, we can find the density profile of the locally phase-separated brush both for the dilute tail and the condensed region of the brush. In the analytical model these density profiles are found from eq 21, by inverting $u[\rho_p]$. In the numerical model the rather complex self-consistent field equations must be solved as explained above in the numerical model. The results of the two approaches are plotted in Figure 3. The chain length used in the numerical model is $N = 200$, which is relatively short. In both models we have used $m = 1$, which means that each polymer unit is an acid group. The pH is such that $\mathrm{pH} - \mathrm{p}K = 1$ or, equivalently, $\alpha_b = 0.9$. We have chosen for a relatively bad solvent $\chi = 2$. From Figure 2 we should expect that in this case the tail of the profile has a reasonably high density. We further fixed the grafting density σ to 0.03 chains per unit area. With the σ parameter one can adjust the volume of the condensed part of the internally phase-separated brush. Even when the ionic strength is not

very low, (in this example $\Phi = 0.01$) the brush is characterized by a very long tail extending up to 50% of the full length of the polyelectrolyte chain. This height is only a very weak function of the grafting density (not shown). On the other hand, the thickness of the collapsed part is very sensitive to σ. Note that, when the size of the condensed part is less than the square root of the chain length, the brush is unstable against lateral fluctuations. This can happen most easily for short chains, and thus we expect in practical cases a lateral inhomogeneous layer once the brush is collapsed. Lateral inhomogeneities are not studied in the present paper.

Inspection of Figure 3a shows that excellent agreement is found for the overall segment density profile, which shows that chains with a length of $N = 200$ can be considered sufficiently large. There are only noticeable differences between the numerical result and the analytical one in those parts of the profile where the density changes abruptly and also at the brush boundaries. These differences are caused by the fact that in the numerical calculations the chain length is very small. Then fluctuations not included in the most likely trajectories of the analytical approach will give rise to a "tail" at the end of the profile. In this tail the relative influence of the deviations from local electroneutrality is still noticeable, as will be discussed below in more detail. Both the density of the brush on the condensed side of the brush and that in the dilute part are well-predicted by the asymptotic relations, which shows that the phase diagram of Figure 2 has indeed predictive power with respect to the density jump in the brush.

In Figure 3b we present the distribution of the free ends of the tethered chains as a function of the normalized coordinate z. In the analytical model it is possible to find an expression for this quantity as explained in the Appendix. It is important to note that both approaches show that the end-point distribution has two maxima, one in the condensed part of the profile and one in the dilute part. In the numerical model the end-point distribution is continuous, but in the analytical theory, a singular value is found at the edge of the condensed part of the brush. From eq A5 the order of this singularity can be found. When the density profile shows a jump, we have

$$\frac{\partial \rho_p(u)}{\partial u} \sim \Delta\rho_p \delta(u - u_b) + \text{nonsingular terms} \quad (26)$$

where $\Delta\rho_p$ is the density jump from the high density in the condensed part to the low density in the dilute part of the profile and u_b is the exchange chemical potential at this point. Inserting eq 26 into eq A5 we find:

$$g(z) = \frac{a\sqrt{2}}{\sigma\pi} \frac{\theta(z_b - z)\Delta\rho_b \sin\dfrac{\pi z}{2}}{\sqrt{\cos^2\dfrac{\pi z}{2} - \cos^2\dfrac{\pi z_b}{2}}} + \text{nonsingular terms} \quad (27)$$

where θ is the Heaviside function. Asymptotic expansion of eq 27 gives the order of the singularity to be

$$g(z) \propto \frac{1}{\sqrt{z_b - z}} \quad (27)$$

This divergence is the reason for the relatively large deviations between the numerical and the analytical theory for the end-point distribution in the condensed region of the brush. The divergence does not occur in systems with finite chain length, and thus in the numerical calculations $g(z)$ remains finite.

Order of the Structural Transition of the Polyelectrolyte Brush. We now examine the phase transition of the brush in more detail. Let us follow the scenario that first the brush is in the dilute side, outside the binodal, and then change the conditions such that we enter into the two-phase region. Thus, let us consider the case where the grafting density is relatively low. The brush is in the swollen state due to the charges along the chain. The density at the lower branch $\rho^{(1)}_p$ of the binodal exceeds the density of the brush at $z = 0$, $\rho_p(0) < \rho^{(1)}_p$. We can now increase χ, decrease pH, increase Φ, or increase the grafting density to move the polymer density toward the binodal value: $\rho_p(0) \rightarrow \rho^{(1)}_p$. At the transition point, when , $\rho_p(0) = \rho^{(1)}_p$, an infinitely thin layer of the condensed phase starts to develop. Now, at the interface the density of the polyelectrolyte is equal to the density corresponding to the upper branch of the binodal , $\rho_p(0) = \rho^{(2)}_p$. The appearance of a new phase with a substantially different density at the transition point is typical of a first-order phase transition. In the analytical model, formally the limit to infinite chain length is taken. In terms of the normalized distance z, the transition at the surface is taking place in an infinitely small part of the system. In the analytical model the contribution of this ultrathin layer to the free energy will therefore be very small and the collapse of the polyelectrolyte brush will tend to be a continuous transition. Thus, in the limit of infinitely long chains, the phase transition will be second-order.

For finite chain lengths, however, the problem is more involved. First of all, the thickness, $\delta^{(2)}$, of the collapsed part of the layer should not be less than the Gaussian size of the polymer chain in the brush in order to remain laterally homogeneous. Thus $\delta^{(2)} \geq a\sqrt{N}$. As the height of the brush is proportional to N, the relative thickness of the collapsed layer at the transition point can go to zero when $N \rightarrow \infty$. For finite chain lengths, the condition $\delta^{(2)} \geq a\sqrt{N}$ is not automatically fulfilled. Furthermore, the jump of the segment density in the brush from the condensed phase to the swollen phase will cause a jump of the electrostatic potential and the appearance of an electric double layer. With the manifestation of the electric double layer, a finite free energy contribution should be added to the system. Again, for finite chain lengths this contribution will not be automatically small. The energy of this electric double layer has to be compensated for by free energy benefits of the condensed phase. In effect it should be possible that for polyelectrolyte brushes with finite chain lengths the transition is first-order.

In Figure 4 the normalized average height is plotted as a function of the grafting density for conditions similar to the ones chosen in Figure 3. In this graph the analytical result for infinite chain length is given by the dashed curve. We see that, as discussed above, there is no jump in the average height in the analytical theory. Instead, a break is found in the curve for the average height z_{rms} as a function of the grafting density. For high grafting density the average height is including both the condensed part and the dilute part of the brush and z_{rms} is small. In low grafting densities it is just determined by the density profile of the swollen tail, giving a high value for z_{rms}. We do not find any hysteresis at low ionic strength, but clearly we have one

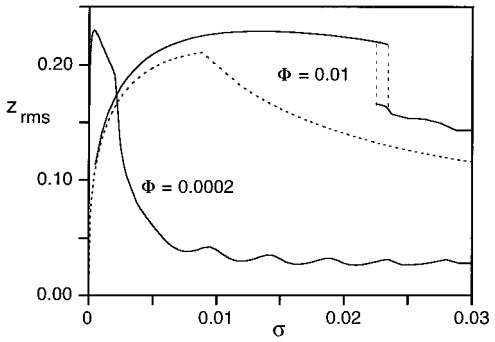

Figure 4. Normalized average height for a polyelectrolyte brush as a function of the grafting density σ for the numerical model ($N = 200$ and $\Phi = 0.01$ or $\Phi = 0.0002$) (solid curves) and for the analytical asymptote for $\Phi = 0.01$ (dashed curve). Other parameters: $\alpha_b = 0.9$, $\chi = 2$, $m = 1$. The vertical dashed lines indicate the hysteresis region as found in the numerical calculations.

for the higher ionic strength case (in the numerical result). Most probably, the reason that there is no jump at low ionic strength is that too little material is present in the brush to have the jump in density. The transition occurs near a grafting density of 0.002, which corresponds to only 0.4 equivalent monolayers of material in the brush. It is expected that for longer chains the height will be discontinuous with σ, but in the limit of $N \rightarrow \infty$, this jump should be absent again. At present, the numerical calculations for chains much longer than $N = 200$ are extremely time-consuming. The jump in the average height found for $\Phi = 0.01$ occurs at considerably higher grafting density (approximately 4 equivalent monolayers).

Typically, we find in the σ range below the transition a maximum in the average height of the brush. This maximum is similar to that found for the polyacid brush in good solvents. For very low grafting densities, the brush is below the overlap condition and naturally the brush height increases with increasing σ. For higher grafting densities the height reduces with increasing σ. This is because the chains feel each other electrostatically, and they adjust their local degree of dissociation, which diminishes the swelling. Part of the brush (near the surface) has a profile corresponding to that of a neutral brush. For high grafting densities, for values larger than the critical grafting density where the transition takes place, first the height of the brush continues to go down, but as soon as the condensed part dominates the height characteristics, z_{rms} becomes proportional to σ (not shown). The oscillations found in this part of the curves are due to lattice artifacts. As the brush is of the form shown in Figure 3, there is a sharp interface between the condensed part and the swollen part. The growth of the condensed part is in principle continuous, but in a lattice model, some values of the thickness of the condensed part are more favorable than others, and we see in the lattice model an oscillation for each amount of polymer with which the thickness grows with one lattice layer.

It is interesting to compare in Figure 4 the analytical asymptotic prediction with the numerical results for finite chain length in the context of the speculations about the order of the phase transition given above. We see that both at very low and at high grafting densities the average height behaves very similarly in the numerical calculations and the analytical asymptote. Only near the jump in height are there deviations between the two cases. The break in the curve in the analytical approach occurs at a smaller σ than the jump in the numerical result. This is completely in line with the extra amount of energy needed to create the interface between the condensed and the swollen part of the profile. It is natural that due to this effect the transition is postponed slightly.

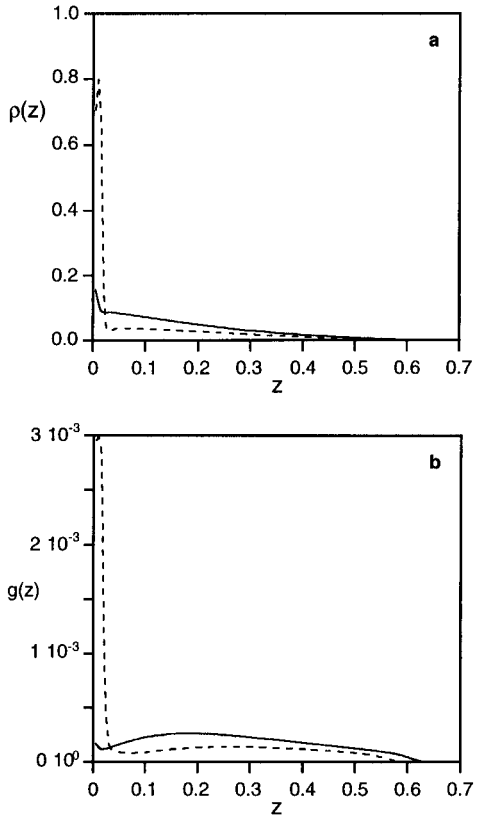

Figure 5. (a) Overall density of the brush as a function of the normalized distance z. (b) The end point density as a function of the normalized distance z. The conditions are chosen in the hysteresis region of Figure (4). The solid curves correspond to the swollen layer (upper branch in Figure (4), and the dashed curve to the phase-separated brush (lower branch). Parameters: $N = 200$, $\Phi = 0.01$, $\alpha_b = 0.9$, $\sigma = 0.0225$, $\chi = 2$, $m = 1$.

Obviously, not only the height of the brush jumps at the transition, but also many other structural parameters suddenly change. As can be seen in Figure 4, a hysteresis is found in the numerical result . This means that for one grafting density we have two different solutions for the structure of the brush. These two solutions were generated by our numerical method by making small steps in σ and using the previous solutions of the set of equations for the next grafting density. In this way, we were able to stay for some time on the upper or lower branch, even when the other branch would have been energetically more favorable. The exact transition point was not calculated, but it can be found by equating the free energy per chain in both branches of the hysteresis region.

In Figures 5−7 we examine the structure of the layer in detail. We compare the properties of the brush corresponding to the upper branch and the lower branch in the jump region. Thus the two types of brushes to be discussed both have the same number of chains per unit area, and all other parameters are also identical.

In Figure 5 we present the structure of the brush in a way similar to Figure 3. Here we compare the structural properties of the brush in the two-phase region (solid curves) with the situation that the brush

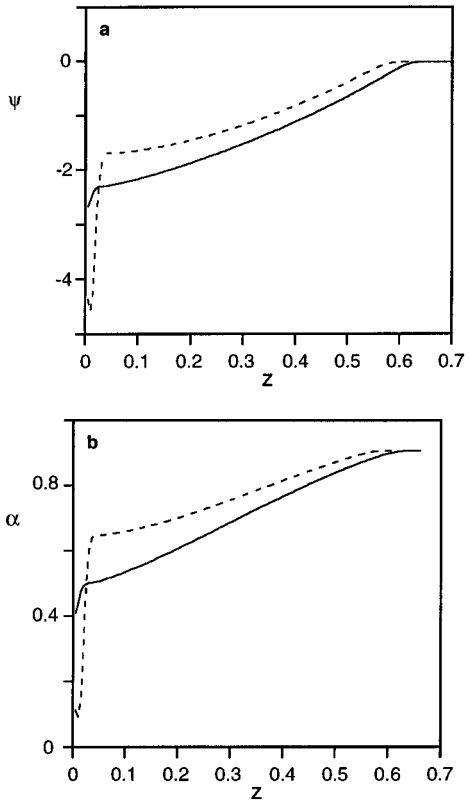

Figure 6. (a) Electrostatic potential as a function of the normalized distance z. (b) Degree of dissociation as a function of the normalized distance z: solid curve, swollen layer, dashed curve, phase-separated layer. Other parameters are as in Figure 5.

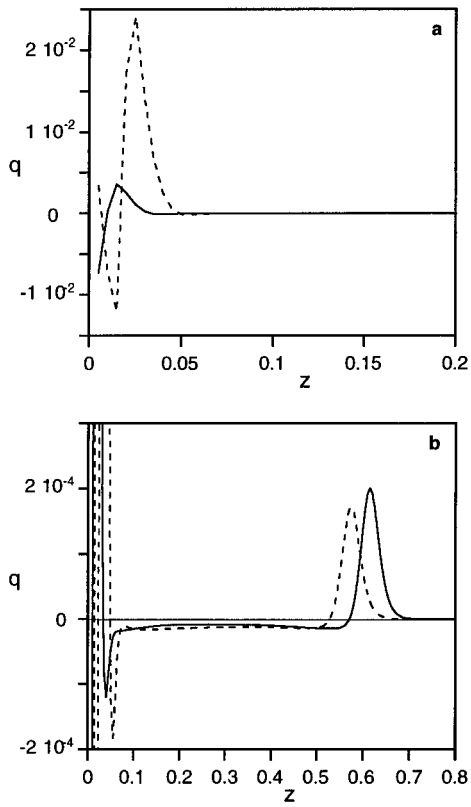

Figure 7. Excess charge as a function of the normalized distance *z* on two levels of magnification. In view a, only the inside of the brush is given. In view b, we have expanded the *q* scale and show also the outer part of the brush. Parameters are as in Figure 5.

is still in the swollen state (dashed curves). Only the numerical results are presented. The overall structure and the end-point distributions have exactly the same features as discussed in Figure 3. The brush in the swollen state corresponds more or less to the swollen tail of the phase-separated system. Near the surface there is a small increase in density which may be interpreted as a pretransition structure. Also, the shift of the maximum of the end-point distribution in Figure 5b to rather low *z* may be interpreted in this way. Due to the finite thickness of the boundary between the condensed and swollen part of the brush, the density in the swollen layer does not necessarily equal that of the binodal value as given in Figure 2. Nevertheless, this density is very close to the binodal value, as is easily seen by comparison of Figure 5 with Figure 3.

The dimensionless electrostatic potential profile (a value of $\psi = -1$ corresponds to -25 mV) and the local degree of dissociation are plotted as a function of the normalized distance *z* in Figure 6. Due to the reduced coordinates we see that the diffuse part of the double layer outside the brush is relatively small. Thus, the potential as a function of *z* shows a rather sharp break at the end of the brush. The electrostatic potential is negative inside the brush because the polymer units have a negative charge. In the swollen part of the profile both the swollen layer and the phase-separated layers have approximately the same electrostatic potential profile. Obviously, in the condensed part of the profile the potential jumps to a more negative value rather abruptly. We note that apart from the polymer−solvent and the excluded volume interactions (i.e., the factor $\gamma(x)$ in eqs 2 and 3), the electrostatic potential is the distribution function for the free ions. Only in the condensed part of the profile are the solvent quality and excluded volume of the ions important. The degree of dissociation closely follows the profile of the electrostatic potential. The value is 0.9 when the electrostatic potential is zero, and the value is smaller when the potential is negative. Obviously in the condensed part of the brush the degree of dissociation is very low.

The excess charge profile in the polyelectrolyte brush is in principle rather uninteresting. As a first approximation, the charge is zero throughout the layer. However, in the numerical model for not extremely high chain length, we expect some build-up of charges in the interfacial zones in the profile. Indeed, a rich behavior of the excess charge as a function of the normalized distance is found as given in Figure 7. Let us first discuss the features of Figure 7a, where the charge density is plotted on a 10^{-2} scale. We can deduce that in the interfacial zone only about 10% of the charges of the brush are not compensated. As anticipated above, we expect an electric double layer in the region where the brush goes from high density to low density. Thus, the dashed curve shows an oscillation and can be considered as the derivative of a δ function caused by a break in the electrostatic potential. In the brush corresponding to the one-phase system (solid curve), the charge profile near the surface is somewhat complicated. As the polymer chains have no affinity for the surface, apart from the grafting condition, a small depletion layer develops wherein counterions can sit. This causes the more complicated *q* profile near the surface in this case. When we expand the scale by a factor of 100, we can see the more salient features of the charge profile of the brush. This is given in Figure 7b. Three things

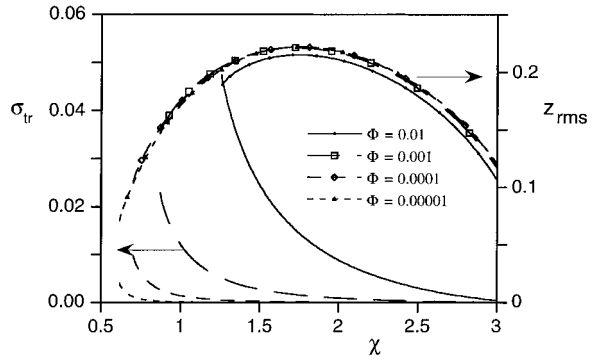

Figure 8. Grafting density and average height of the swollen part of the brush at the transition condition as a function of the Flory−Huggins interaction parameter (inverse temperature) as found by the analytical model. The marked lines correspond to the average height. The ionic strength is indicated. Other parameters: $m = 1$, $\alpha_b = 0.9$.

are worth noting. (i) We observe near the surface the expanded behavior as in Figure 7a. As discussed above there is a break in the electrostatic potential at the outer edge of the profile. The second derivative of this results in a δ function. The remainder of such a δ function is seen near the end of the brush, both in the swollen and in the phase-separated case. (ii) Close inspection of the charge distribution near the transition zone shows that there is some sign of a depletion zone of the swollen part of the chain. This causes the excess charge to show a peak downward. (iii) Apart from the edge effects, we find that in the swollen part of the brush the excess charge is not exactly zero. Instead the charge is relatively constant and slightly negative. This is consistent with the build-up of the electrostatic potential in this part of the brush. This was anticipated above, where it was argued that the magnitude of the excess charge should be inversely proportional to square of the length of the chains.

Finally, in Figure 8 we have collected some characteristics of the transition point as predicted by the asymptotic analysis. In Figure 4 we found the grafting density and height of the transition point at a fixed value of the interaction parameter. In Figure 8 the transition points are given as a function of the inverse temperature for various ionic strength conditions, for the case $\alpha_b = 0.9$ and $m = 1$. The transition height goes through a maximum and the grafting density at the transition point is a decreasing function of χ. In Figure 4 we explained why the height as a function of the grafting density can go through a maximum at relatively low grafting density. This maximum is a clear signature of a polyacid chain (annealed case). The decrease of the height with increasing grafting density is at first sight a rather unexpected behavior, which can be explained by the reduction of the degree of dissociation of the chains with increasing grafting density. The transition point as given in Figure 8 can now be either on the rising or decreasing part of the behavior of the height as a function of the grafting density, which explains the maximum in Figure 8. The trend found for the grafting density at the transition point is much easier to explain. It is rather obvious that, when the solvent becomes worse, the transition should take place at lower grafting density. It is interesting to note that the ionic strength is not important for the height at the transition point, but it does influence strongly the critical grafting density. This dependence is consistent with the binodal data presented in Figure 2.

Conclusions

Polyelectrolyte brushes and, consequently, polyelectrolyte systems under poor solvency conditions are extremely rich objects from a physical−chemical point of view. We have proven that internal phase separation may be found, which can occur as continuous (second-order) or jump-like (first-order) phase transitions. For systems with a finite chain length, we expect that, when the thickness of the condensed part of the brush is less than the characteristic size of the coil in solution, the layer will be laterally inhomogeneous. The conditions necessary to find these transitions are well within the experimental range.

The structure of polyelectrolyte brushes as a function of the electrolyte concentration and solvent quality is nontrivial. Often, a long dilute tail is found with a size which is only slightly smaller than the full length of the chain. This has important implications for problems related to the colloidal stability.

Acknowledgment. V.A.P acknowledges the hospitality of the Department of Physical and Colloid Chemistry of the Agricultural University of Wageningen. This work was also partly supported by INTAS Grant No. 93−3372. V.A.P. acknowledges the Russian Foundation for Basic Reseach (Grant 96−03−33862) for financial support.

Appendix

By virtue of the definition of a brush (see the review by Milner[26]), the height of the brush is proportional to the length of the chains. In this structure the polymer chains are strongly stretched. The usual approximation for a stretched polymer chain in a brush is to present such a chain as a spring with nonlinear elasticity.

We consider chains[18] with length N stretched by a force $f = pkT/a$ applied to the ends of the chain. The extensibility of the chain is defined by the increment of the average elongation, $\langle \delta x(p) \rangle$, obtained by an increment of the chain length, δN, under the applied stretching force, p:

$$e(p) = \frac{\langle \delta x(p) \rangle}{a \delta N} = \frac{\mathrm{d}\{\ln Z(p)\}}{\mathrm{d}p} \tag{A1}$$

where $Z(p)$ is the partition function per segment of the chain with the condition that the dimensionless stretching force, p, is applied to the ends of the chain.

On each segment a dimensionless force is present. When the chains are end-tethered, the problem becomes one-dimensional. There exists a potential $V(z)$ from which it is possible to obtain the force p. In the brush, $V(z)$ will be related to the local segment chemical potential, u, as used above. We will first analyze the case of an arbitrary $V(z)$. The system of equations that describe the static equilibrium of the sth segment of the polymer chain in dimensionless form is

$$\left.\begin{aligned} \frac{\mathrm{d}p}{\mathrm{d}l} &= -\nabla V(z) \\ \frac{\mathrm{d}z}{\mathrm{d}l} &= e(p) \end{aligned}\right\} \tag{A2}$$

where z is the average position of the sth segment, $l = s/N$, and $z = x/(aN)$. The corresponding boundary conditions are $z(l)|_{l=0} = 0$, $p(l)|_{l=1} = 0$. The integral of the system of differential equations given by eq A2 is $Z(p) = \exp(V(z_e) - V(z))$, where z_e is the most probable height of the free end of the chain. The value of z_e is

determined from the equation

$$1 = \int_0^1 \mathrm{d}l = \int_0^{z_e} \left(\frac{\mathrm{d}z}{\mathrm{d}l}\right)^{-1} \mathrm{d}z = \int_0^{z_e} \frac{\mathrm{d}z}{e\{Z^{(-1)}[\exp(V(z_e) - V(z))]\}}$$

Now we can define the local density of the segments of the chain in the stretching field $V(z)$:

$$\rho(z,z_e) = \frac{\mathrm{d}l}{\mathrm{d}z} = \frac{1}{e\{Z^{(-1)}[\exp(V(z_e) - V(z))]\}}$$

where $\rho(z,z_e)$ is the density at coordinate z generated by the chains started at z_e. One can see that $\rho(z,z_e)$ is a monotone increasing function of z. In the thermodynamically stable systems $u[\rho]$ is an increasing function of ρ. It is significant that to obtain the stretching of the chain, $u[\rho(z)]$ has to be a decreasing function. Consequently, $\rho(z)$ also has to be decreasing function with z.

The only possibility to provide continuous distribution of the free ends of the monodisperse chains in the brush is to use the potential allowed for this distribution (so-called indifferent equilibrium).

The equation for this potential $V(z)$ is found by a so-called "equal time" condition:

$$\int_0^{z_e} \frac{\mathrm{d}z}{e\{Z^{(-1)}[\exp(V(z_e) - V(z))]\}} = 1 \;\forall\; z_e \qquad \text{(A2)}$$

The Laplace transformation by V is (see the ref 18 for more details):

$$\int_0^1 \exp(-\omega V(z))\,\mathrm{d}z \int_0^\infty Z(p)^\omega \,\mathrm{d}p = \frac{1}{\omega} \qquad \text{(A3)}$$

The profile of the potential is independent of the interaction between the chains in the brush. If $u[\rho]$ is changed the density profile $\rho(z)$ will also change, and when $\rho[u]$ is changed, the same will happen with $u(z)$. The invariance of $u[\rho(x)]$ (SCF) determines the structure of the brush.

The density profile $\rho(z)$ can be calculated from the equation of self-consistency:

$$\left.\begin{aligned} u[\rho(z)] &= \Lambda - V(z) \\ \int_0^{z_{max}} \rho(z)\,\mathrm{d}z &= \sigma \end{aligned}\right\} \qquad \text{(A4)}$$

where σ is the surface grafting density.

Of special interest, the distribution of the free ends can be obtained. By virtue of the definition of this distribution function, we must have

$$\rho(z) = \sigma \int_z^{z_{max}} g(z_e)\rho(z,z_e)\,\mathrm{d}z_e \qquad \text{(A5)}$$

The inversion of this equation is

$$g(z) = \frac{1}{\sigma}\frac{\mathrm{d}V}{\mathrm{d}z}\int_{V(z)}^{V(H)} \frac{\mathrm{d}\rho(v)}{\mathrm{d}v}\,\xi(V(z') - v)\,\mathrm{d}v \qquad \text{(A6)}$$

where $\xi(V) = \mathrm{d}z(V)/\mathrm{d}V$. $\rho(u)$ is defined by inversion of eq A4 and $z(v)$ is defined as $V(z(v)) = v$.

We find the class of the analytical solution of eq A3. If $Z_a(p) = \cosh^\beta(cp)$, we have

$$V_a(z) = -\beta \ln \cos\frac{\pi z}{2c\beta} \qquad \text{(A7)}$$

One can see that $Z(p)$ for the freely joined polymer chains on the square (SL), diamond (DL), and body centered cubic (BCC) lattices have this form. This allows us to calculate the analytical expressions for the structure of the brushes of these polymer chains.

The free ends distribution for the case of BCC is

$$g(z) = \frac{a\sqrt{2}}{\sigma\pi}\tan\frac{\pi z}{2}\int_A^B \frac{\mathrm{d}\rho_p(v)}{\mathrm{d}u}\frac{\exp(v/3)\cos(\pi z/2)}{\sqrt{1 - \exp(2v/3)\cos^2(\pi z/2)}}\,\mathrm{d}v \qquad \text{(A8)}$$

where

$$A = -3\ln\cos\left[\frac{\pi z}{2}\right] \qquad B = -3\ln\cos\left[\frac{\pi}{2}z_{max}\right]$$

References and Notes

(1) Alexander, S. *J. Phys. (Paris)* **1977**, *38*, 983.
(2) Halperin, A.; Tirrell, M.; Lodge, T. P. *Adv. Polym. Sci.* **1991**, *100*, 31.
(3) Cohen Stuart, M. A.; Fleer, G. J.; Lyklema, J.; Norde, W.; Scheutjens, J. M. H. M. *Adv. Colloid Interface Sci.* **1991**, *34*, 477−535.
(4) Zhulina, E. B.; Borisov, O. V.; Priamitsyn, V. A. *J. Colloid Interface Sci.* **1990**, *137*, 495.
(5) Israëls, R.; Leermakers, F. A. M.; Fleer, G. J.; Zhulina, E. B. *Macromolecules* **1994**, *27*, 3249.
(6) Lyatskaya, Y. V.; Leermakers, F. A. M.; Fleer, G. J.; Zhulina, E. B.; Birshtein, T. M.; *Macromolecules* **1995**, *28*, 3562−3569.
(7) Misra, S.; Mattice, W.; Napper, D. *Macromolecules* **1994**, *27*, 7090.
(8) Ross, R.; Pincus, P. *Macromolecules* **1992**, *25*, 2177.
(9) Zhulina, E. B.; Birshtein, T. M.; Borisov, O. V. *Macromolecules* **1995**, *28*, 1491−1499.
(10) Leermakers, F. A. M.; Atkinson, P. J.; Dickinson, E.; Horne, D. S. *J. Colloid Interface Sci.* **1996**, *178*, 681−693.
(11) de Kruif, C. G.; Zhulina, E. B. *Colloid Surf. A.* **1996**, accepted.
(12) Israëls, R.; Leermakers, F. A. M.; Fleer, G. J.; Zhulina, E. B. *Macromolecules* **1994**, *27*, 3249.
(13) Borisov, O. V.; Birshtein, T. M.; Zhulina, E. B. *J. Phys. II* **1991**, *1*, 521.
(14) Fleer, G. J.; Scheutjens, J. M. H. M.; Cohen Stuart, M. A.; Cosgrove, T.; Vincent, B. *Polymers at Interfaces*, Chapman & Hall: London, 1993.
(15) Scheutjens, J. M. H. M.; Fleer, G. J. *J. Phys. Chem.* **1979**, *83*, 1619−1635.
(16) Scheutjens, J. M. H. M.; Fleer, G. J. *J. Phys. Chem.* **1980**, *84*, 178−190.
(17) Semenov, A. N. *Sov. Phys. JETP* **1985**, *61*, 733.
(18) Amoskov, V. M.; Pryamitsyn, V. A. *J. Chem. Soc. Faraday Trans.* **1994**, *90*, 889−893.
(19) Amoskov, V. M.; Pryamitsyn, V. A. *Polym. Sci. Russ.* **1995**, 37A.
(20) Evers, O. A.; Scheutjens, J. M. H. M.; Fleer, G. J. *Macromolecules* **1990**, *23*, 5221.
(21) Vincze, A.; Horvai, G.; Leermakers, F. A. M. *J. Phys. Chem.* **1996**, *100*, 8946.
(22) Zhulina, E. B.; Pryamitsyn, V. A.; Borisov, O. V. *Polym. Sci. USSR* **1989**, *31*, 205.
(23) Zhulina, E. B.; Borisov, O. V.; Pryamitsyn, V. A. *J. Colloid Interface Sci.* **1990**, *137*, 495.
(24) Wijmans, C. M.; Scheutjens, J. M. H. M.; Zhulina, E. B. *Macromolecules* **1992**, *25*, 2657−2665.
(25) Milner, S. T.; Witten, T. A.; Cates, M. E. *Macromolecules* **1988**, *21*, 2610.
(26) Milner, S. T. *Science* **1991**, *251*, 905.

MA9607832